Macromolecules
ARTICLE

Macromolecules **2010**, *43*, 5561–5568 **5561**
DOI: 10.1021/ma1006599

Online Low-Field ^{1}H NMR Spectroscopy: Monitoring of Emulsion Polymerization of Butyl Acrylate

Maria A. Vargas,[†] Markus Cudaj,[‡] Kidist Hailu,[†] Kerstin Sachsenheimer,[†] and Gisela Guthausen*,[†]

[†]*Karlsruher Institut für Technologie (KIT), Institut für Mechanische Verfahrenstechnik und Mechanik (MVM), SRG10-2, 76131 Karlsruhe, Germany, and* [‡]*Karlsruher Institut für Technologie (KIT), Institut für Technische Chemie und Polymerchemie, D-76128 Karlsruhe, Germany*

Received March 26, 2010; Revised Manuscript Received May 14, 2010

ABSTRACT: The emulsion polymerization of butyl acrylate was monitored by online nuclear magnetic resonance spectroscopy at 20 MHz ^{1}H frequency. The reaction progress could be followed, monitoring the conversion of the reactant time-resolved without any need of sample preparation. Experimental data were analyzed with kinetic models for free-radical polymerization. The data comprised the polymerization rate in seeded batch emulsion polymerizations of butyl acrylate with doubly deionized water and D_2O as solvent. The polymerization rate versus conversion curve behaves compatible with the three rate intervals model, typically observed in emulsion polymerizations. Zero−one kinetics explains the experimental results appropriately, leading to the determination of entry and termination rate coefficients.

1. Introduction

The synthesis of a polymer is a complex process that produces material of a quality that is dependent on reaction conditions. The corresponding reactor models are often complicated and require numerous parameters and pseudoconstants.[1−9] The situation is even more difficult in emulsion systems. A time-resolved measurement of monomer, particle, and radical concentrations is needed in order to validate theoretical models and to provide experimentally determined coefficients that enter the models.

Process and product variables related to end-use polymer properties are often measurable only with poor time resolution or not at all. Thus, for the polymerization process, product quality monitoring and control are challenging tasks.[10−19] Few reliable and flexible approaches for the measurement of monomer conversion are known in the literature.[10,11,15−17] Thus, the design of new analytical methods remains an active field of research.[11,12,16,17,19]

Online methods for measuring chemical and physical properties of polymerization reactions are advantageous because they provide a direct process control also in industrial applications without sampling during the reaction.[14−16,20] Examples for online capable measurement techniques for emulsion polymerization[8,10−22] are calorimetry, chromatography, densitometry, dielectric spectroscopy, electrical conductivity, turbidity measurements, and ultrasound propagation. Challenges are still in the online control of conversion and molar mass,[11,15,17,19] in the derivation of interesting parameters for description of the complex process mechanisms, and finally in the feedback from the experimental findings for an operation with optimized reaction parameters.

For online studies in engineering applications under process conditions, the nearly non-invasive NMR spectroscopy can be a powerful method that provides unique information about morphological and dynamic properties of polymer particles by taking advantage of the high selectivity of the method to details of chemical structure[13−15,20−22] and molecular dynamics. Also, NMR spectroscopy allows the investigation of the reaction process almost in real time under process conditions in a wide range of temperature and pressure.[14−16] In the present study, the reaction is investigated at a low magnetic field with its special challenges.[15,16,21]

From chemical engineering point of view, *n*-butyl acrylate (BA) is a monomer commonly used in acrylic formulations, and considerable effort has been devoted to study its emulsion polymerization.[1−5,20,23−33] However, the knowledge of the effect of process variables on kinetics and molar weight distribution (MWD) is scarce.[2,3,5] Because of the heterogeneous nature of an emulsion polymerization and the concomitant large number of kinetic events, data analysis and determination of kinetic constants are rather complicated. Nevertheless, it has been shown that one may obtain unique (and frequently over determined) values for all relevant rate parameters by a combination of the available data.[2,8,26−28,30,33]

An important aspect is to define two limits or categories to describe emulsion polymerization kinetics, which are the zero−one and pseudobulk kinetics, as approximations to the "true" kinetics.[7,8,20,23,28,33−41]

For mathematical modeling,[1,8,22,29−31] the knowledge of the propagation rate constant is required among other kinetic parameters. The IUPAC Working Party "Modelling of Kinetics and Process of Polymerization" has made considerable effort to obtain consistent values for the propagation constants (k_p). The measurement of k_p by PLP (pulsed laser polymerization) has encountered some difficulties for monomers such as BA.[1,7,22,24,29,33,40]

The purpose of this work is to obtain the rate coefficients by online measurements of low-field ^{1}H NMR spectroscopy for monitoring the emulsion polymerization of butyl acrylate. For this aim, the decreasing signal of the olefinic double bond in butyl acrylate as well as the growing signal of the newly formed saturated polymer main chain is followed in addition to the polymer chain dynamics by line width analysis. Experimental data of rate parameters can be compared with predictions from models in order to elucidate whether the emulsion polymerization

*Corresponding author: Tel +49 (0)721 6088058, e-mail gisela.guthausen@kit.edu.

Published on Web 06/02/2010

of BA can be described by a zero−one model from the viewpoint of the NMR experiment.

2. Experimental Section

2.1. Reagents and Reagent Purification. Distilled deionized water was used in one polymerization reaction and D_2O (90 atom % D), purchased from Armar Chemicals (Switzerland), in the other. The emulsifier, sodium dodecyl sulfate (SDS, ≥99%, Sigma-Aldrich, Germany), initiator ($(NH_4)_2S_2O_8$, ≥99%, Roth, Germany), and buffer ($NaHCO_3$, ≥99,5% p.a. Roth, Germany) were used as supplied without further purification. BA (purity ≥99%) was purchased from Sigma-Aldrich, Germany.

2.2. Online Low-Field NMR Spectroscopy. The experimental setup for online ^{1}H NMR reaction monitoring consists essentially of a low-field NMR (20 MHz) spectrometer and a flow system. The NMR spectrometer is based on a commercially available mq20 minispec (Bruker, Germany), which was adapted for spectroscopy. The probe comprises a lock substance externally to the flow cell, which has the function of frequency correction and feedback during the experiment. It is independent of the flow system. Additionally, this construction allows a direct monitoring of the reproducibility of the NMR spectra by recording the reference signal coincidently with the reactant's spectrum. Besides the lock, an electrical shim system was built into the probe, equipped with 12 orders plus a B_0 correction term for improvement in B_0 homogeneity such that the full width at half-height of a single NMR peak amounts to about 0.2 ppm in a cylindrical volume of about 5 mm × 15 mm. For polymer reactions and other relatively simple chemical reactions, this resolution is sufficient for answering questions like reaction progress and conversions of specific moieties. The flow system consists of a silicon rubber tube, a Teflon (PTFE) tube, fed through the NMR probe, and a syringe pump, which pumps the reactant liquid in a closed loop bypass directly through the NMR spectrometer and back into the reactor. The Teflon tube has the advantage that poly(BA) does not stick into it in the course of the reaction, where it does in the silicon rubber tube. The contactless pumping by the syringe pump (Watson Marlow Sci. 323, England), however, requires the usage of the silicon rubber hose. The contactless pumping is especially useful in the present reaction because of the cluing properties of poly(BA) and the oxygen sensitivity. Flow rates (50 rpm), diameter, and length of the tubes had to be optimized taking into account the requirements of flow NMR experiments as well as the changing sample and environmental properties. The NMR sequence was a single-pulse experiment with a pulse length of 7.5 μs; the acquisition time amounted to 400 ms. The probe and receiver dead time was 20 μs. Thirty-two scans were added with a recycle delay of 0.9 s. A waiting time of 60 s was chosen between the repeated experiments. Care was taken that the thermal magnetization equilibrium state was reached by observing subsequent scans. The effective T_1 for the flowing system is smaller than the measured T_1 for a static sample due to inflow effects during the recycle delay, such that the experiment could be essentially repeated at T_1. The relatively small flow rate allows a complete polarization of the liquid during passing through the magnet which has a diameter of 125 mm. Therefore, no special premagnetization region was needed for these experiments. The spectra were referenced to the external capillary sample in the probe, which allows a direct and sample independent calibration of the frequency axis. Additionally, the signal amplitude of the intrinsic reference can be used for monitoring the quality and stability of the NMR measurements.

The recorded spectra were subsequently analyzed by a peak fitting routine written in Matlab, where the lines, expected from the high-field investigations,[20] are described by Gaussian lines with variable width and integrals. As the olefinic and the water shifts are independent of the reaction progress, the shifts of these species are fixed for all spectra. The olefinic signal integral and the aliphatic line width are the important parameters reflecting the reaction progress. They are discussed as a function of reaction time.

2.3. Emulsion Polymerization. Batch emulsion polymerization was carried out in a 350 cm^{-3} five-necked glass reactor equipped with a condenser, a mechanical stirrer having a constant speed of 400 rpm, and a reflux condenser in a total batch period of about 3 h. DDI water (220 cm^{-3}), 0.52 g (6.2×10^{-3} mol) of sodium bicarbonate (buffer), and 2.52 g (8.74×10^{-3} mol) of sodium dodecyl benzenesulfonate (surfactant) were added to the reactor. After 25 min, 98 g (0.77 mol) of butyl acrylate was added, and the reaction temperature was maintained at 70 °C. At the beginning of the reaction, water and emulsifier were added. After dissolution of emulsifier, the monomer was added. Agitation was started while the reactor was purged with nitrogen for about 15 min to deoxygenate the mixture. Subsequently, heating was started. When the reactor content reached the desired temperature, the initiator solution was added 0.43 g (1.9×10^{-3} mol) of $(NH_4)_2S_2O_8$ in 10 cm^{-3} of water. This point was considered as zero reaction time. As described above, the reactants were measured online by low-field ^{1}H NMR spectroscopy for detection and analysis of the reaction progress. The total reaction time was ∼130 min.

To avoid the dominating proton signal of water in the ^{1}H NMR spectra, the reaction was also carried out in D_2O instead of DDI-H_2O. The reaction was started by adding the initiator at reaction temperature, using the same amounts and conditions as in the DDI-H_2O reaction. The D_2O reaction allows a closer look by ^{1}H NMR spectroscopy into the reaction progress as the olefinic signals from the monomer can be determined much more accurately.

3. Kinetics of Emulsion Polymerization: Entry Model[35] and Apparent Polymerization Rate

Commonly, emulsion polymerization is modeled considering the concentration of different moieties. As NMR spectroscopy is a suitable tool for concentration determination, one model[35] is explicitly summarized here and applied to the data. Via the aid of stabilizators, droplets of the monomers are formed which can be understood as a reservoir in the reaction. Therefore, in the continuous, aqueous phase the monomer concentration is assumed to be constant [M_{aq}]. With the addition of the initiator with concentration [I], the reaction starts as the initiator decomposes with an effective rate constant k_d into radicals with concentration [R]. This step of the radical emulsion polymerization can be described by a first-order reaction, where the efficiency is taken into account by regarding the dissociation constant as an effective rate constant k_d. Theses radicals start to react with monomers dissolved in the continuous phase and form monomer radicals with concentration [M_{ini}]. This reaction is regarded as initial propagation characterized by a rate constant $k_{pw,ini}$. It is the beginning of oligomer formation which takes place in the continuous phase characterized by a rate constant k_{pw}. The solubility of longer chain oligomers, however, is small. Therefore, the probability of an oligomeric radical entering a micelle or a droplet has to be considered. An entry coefficient ρ_w is defined for the description of the entrance of oligomer radicals into latex particles. Commonly, the number of repetitive units in the oligomer radical is 2−3 in most publications,[4,35,42] which is also assumed in the present case. Of course, the entrance process will depend on the available number of micelles or particles N_p. The polymerization reaction can also be terminated with a rate constant k_{tw}, when two radicals react with each other. The probability of termination is a function of the total concentration of radicals [T], apart from the rate coefficient. In micelles or latex particles, polymerization proceeds with its own kinetic law, which is discussed later. Maxwell et al. proposed a mathematic formulation[35] of the scenario in the aqueous phase which is used for modeling of the NMR data presented in this work. The following differential equation system describes the

Table 1. Comparison of the Signals in Low-Field and High-Field ^{1}H NMR for (Poly)butyl Acrylate[a]

component	signal low-field ^{1}H NMR (ppm)	signal high-field ^{1}H NMR[b] (ppm)
olefinic part of butyl acrylate	6−6.5, obscured by water	4.8−6.1
aliphatic part of butyl acrylate	maximum at 1.4	0−1.5
aliphatic part of butyl acrylate and poly(butyl acrylate)	maximum at 1.7	0−1.5; 2.1
O−CH_2	obscured by water	3.7

[a] Differences are due to the minor spectral resolution of the low-field instrument. [b] Reference 20.

time-dependent concentrations of the specific moieties.

$$\frac{d}{dt}[I(t)] = -k_d[I(t)] \quad (1)$$

$$\frac{d}{dt}[R(t)] = 2k_d[I(t)] - k_{pw,ini}[M_{aq}][R(t)] \quad (2)$$

$$\frac{d}{dt}[M_1^0(t)] = k_{pw,ini}[M_{aq}][R(t)] - k_{pw}[M_{aq}][M_1^0(t)] - 2k_{tw}[M_1^0(t)][T(t)] \quad (3)$$

$$\frac{d}{dt}[M_2^0(t)] = k_{pw}[M_{aq}][M_1^0(t)] - k_{pw}[M_{aq}][M_2^0(t)] - 2k_{tw}[M_2^0(t)][T(t)] \quad (4)$$

$$\frac{d}{dt}[M_3^0(t)] = k_{pw}[M_{aq}][M_2^0(t)] - \rho_w\frac{N_p}{N_A} \quad (5)$$

$$[T(t)] = [R(t)] + [M_1^0(t)] + [M_2^0(t)] + [M_3^0(t)] \quad (6)$$

This equation system can numerically be solved for example by the Runge−Kutta numerical integration procedure. In our case this was realized by a self-written Matlab program. An adequate solution requires good estimates for the coefficients as the numerical stability of the solution depends critically on these numbers summarized in Table 2. They show a large scatter which might be due to different experimental conditions.

Apart from the reaction in aqueous phase, the polymerization reaction takes place in the latex particles, which grow from the micelles as formed by stabilizator molecules, by the entrance of the oligomer radicals. These reaction steps cannot be followed explicitly by means of low-field NMR spectroscopy in the sense of concentration determination. However, it is well-known that molecular motional modes of a polymer depend on the chain length. On the other hand, especially ^{1}H NMR transverse relaxation T_2 is given by effective dipolar couplings and the motional spectral density, which both obviously change during a polymerization reaction. An estimate of the transverse relaxation can be obtained from the line width of the corresponding peaks in the spectra. Therefore, a model is needed for description of the chain growth inside the latex particles due to increasing oligomer radical concentration $[M_{3,LP}^0]$ in the latex particles: As a detailed insight into the processes is not possible by means of NMR line width analysis, a pseudo-first-order reaction is assumed with an apparent rate coefficient $k_{p,app}$. The polymer radical concentration $[P_x(t)]$ can therefore be described by eq 7, a termination process being implicitly considered via the time dependent radical concentration.

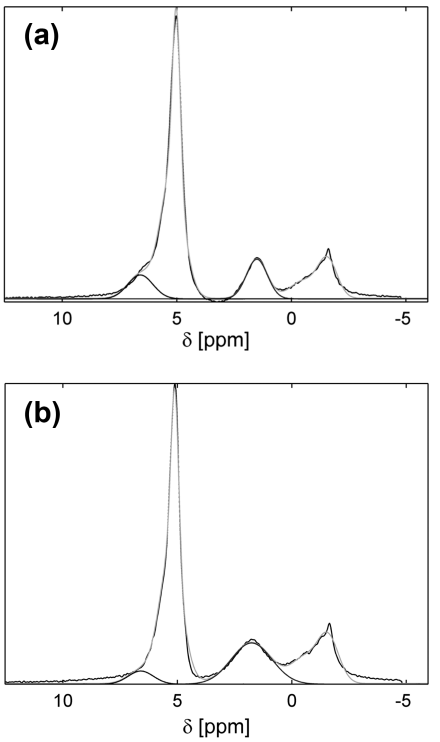

Figure 1. (a) ^{1}H NMR spectrum before polymerization was started using doubly deionized water as solvent. The H_2O peak dominates the spectral signature. Pure butyl acrylate shows a characteristic peak in the olefinic spectral region. (b) After conversion the olefinic signature decreased; the line width especially in the aliphatic spectral region increased once due to an additional line second due to the reduced molecular mobility. The right-hand side line in all spectra corresponds to the external reference in the probe used for lock and reproducibility issues.

$$\frac{d}{dt}[P_x^0(t)] = k_{p,app}[P_{x-3}][M_{3,LP}^0(t)] \quad (7)$$

The integration of this first-order reaction equation leads to an exponential law, which can be fitted to the experimental data, revealing an apparent polymerization rate coefficient for the reaction inside the latex particles.

4. Results and Discussion

4.1. Monitoring of the Reaction by Online Low-Field ^{1}H NMR Spectroscopy. Online detection of emulsion polymerization by ^{1}H NMR allows a relatively short time interval between two subsequent spectra even at the low magnetic field used in this investigation. Figures 1 and 2 show the low-field ^{1}H NMR spectra at about 20 MHz using DDI water and D_2O as solvents, respectively, before the polymerization was started (a) and after completed reaction (b). Monomeric butyl acrylate shows characteristic peaks around 6.5 ppm while poly(butyl acrylate) can be identified by the resolvable signal at 2.1 ppm (aliphatic). The olefinic signal decreases with reaction time as the number of double bonds diminishes. Therefore, the aliphatic signal increases to the same extent. In the work of Landfester,[20] high-field ^{1}H NMR spectra are shown, obtained from an *in situ* MAS experiment. When comparing the spectra (see also Table 1), it is evident that the lines of BA in the range of 4−5 ppm cannot be separated from water in our experiment, but they

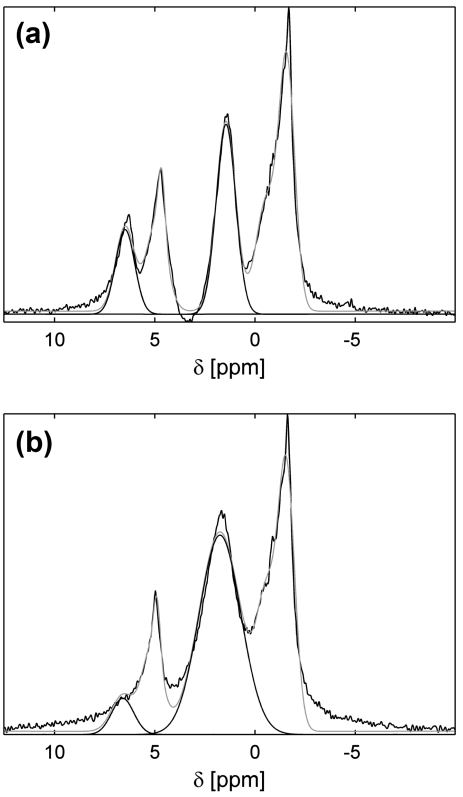

Figure 2. (a) ^{1}H NMR spectrum before polymerization was started using D_2O as solvent. The butyl acrylate monomer shows up more clearly as the water peak is drastically reduced. (b) After the conversion to poly(butyl acrylate) the spectral shape changed (compared with Figure 1): Apart from the decrease in the olefinic region, the line width increased. The line at the right-hand side is again the external reference in the probe.

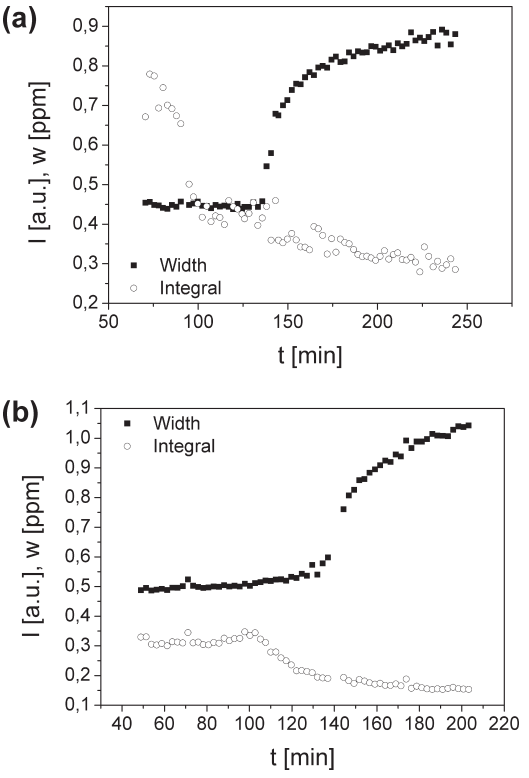

Figure 3. Line width of the aliphatic signal (■) and of the integral of the olefinic signal (○) as a function of reaction time for doubly deionized water (a) and D_2O (b) obtained by online low-field ^{1}H NMR spectroscopy. In (b) the dominating water signal is partially reduced such that the accuracy of the fit to the spectra is superior. The line width starts to increase about 50 min later compared to the onset of the decrease of the olefinic signal. The addition of the initiator was at $t = 50$ min in (a) and at $t = 100$ min in (b).

have to be taken into account in the mass balance. The number of protons in the aliphatic region of the spectrum amounts to 7 per molecule, whereas the number of protons in the olefinic region amounts to 3 per monomer molecule, which is qualitatively reflected in the spectra. In the polymerized state, the olefinic ^{1}H vanishes, and the aliphatic increases by 3 ^{1}H per repeating unit. It is interesting to note the difference in the signal around 4.6 ppm in Figures 1 and 2. Because of the reduced amount of H_2O in this spectral range, the signature of the ^{1}H nearby the oxygen of the acrylic acid of BA in monomer and polymer state can be revealed. Summarizing, the relatively crude picture obtained from the low-field ^{1}H NMR spectra is sufficient to follow the reaction quantitatively online.

Apart from the amplitudes and integrals of specific lines, also line widths can be analyzed. The quantification was done by fitting the spectra by Gaussian lines. According to the definition of the Gaussian function, the half-width σ is defined as line width here. During the reaction, it is found that line width increases, which can be quantified with reasonable accuracy in case of the aliphatic peak. It should be noted that the reaction product shows an NMR line at 2.1 ppm, which could lead to an increase in the line width as the resonances cannot be resolved at the low field and its limited resolution. However, this fact cannot explain the increase in line width accurately as it is much larger and symmetric. It is well-known in polymer ^{1}H NMR spectroscopy that line width, which is related to the transverse relaxation rate, increases as the dipolar couplings increase. This is the case as polymerization progresses: The molecules grow, the molecular motional modes change accordingly, and the sterical arrangements change such that the effective or residual dipolar coupling between nearby ^{1}H increases additionally due to the decrease of the tumbling frequency. Thus, the characteristic increase of the ^{1}H NMR line width is based on an increasing content of polymerized material in the sample which results in a decreasing mobility, i.e., a stronger dipolar coupling. Therefore, line width increases and can be taken as a measure for polymerization progress. Of course, transverse relaxation rate could have been measured spectrally resolved in parallel to the spectra in thermal magnetization equilibrium. However, this additional measurement requires time in the order of minutes leading to only a crude temporal resolution of the online observation of the polymerization.

In Figure 3a, the changes in line width of the aliphatic signature are shown together with the decrease in the olefinic signal intensity for the H_2O-based reaction. As the olefinic signal is dominated by the H_2O signal, the fit is rather incorrect at this spectral region, even more as the line width in the spectra increase significantly during the reaction.

For comparison, the decrease of the olefinic signal integral in case of the D_2O reaction is depicted in Figure 3b again together with the aliphatic line width. As lines are overlapping, the quantification is still inaccurate, especially in case of low olefinic concentrations. Please note that the two experiments were performed subsequently. As the reaction is known to exhibit inhibition times depending for example on temperature and as the fitting accuracy is minor in the H_2O reaction, small time shifts in the results can occur.

4.2. Estimation of Characterizing Parameters of the Emulsion Polymerization. The conversion was estimated from the ratio between the change of the width in the aliphatic spectral

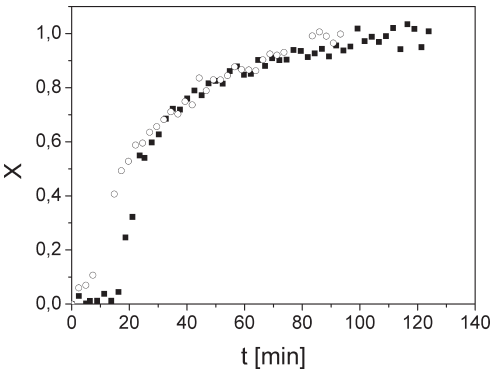

Figure 4. Time evolution of the conversion for butyl acrylate polymerization with water (■) and D_2O (○) as solvent as calculated from the specific line widths in the aliphatic region.

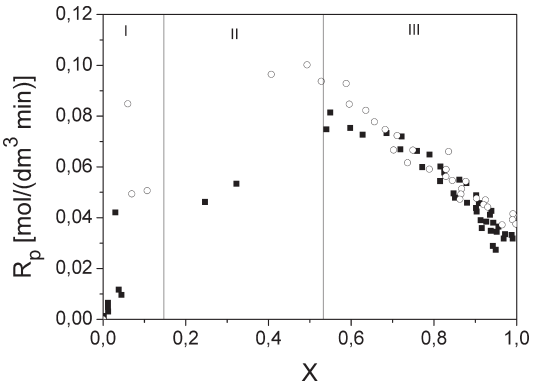

Figure 5. Rate of polymerization (R_p, mol/(dm^3 of water) min^{-1}) vs conversion X for water-based (■) and D_2O-based (○) reactions. The three stages of the emulsion polymerization are indicated on the basis of literature values.[23]

region and the initial BA concentration as a function of reaction time. Figure 4 presents the evolution of the instantaneous conversion of BA. The D_2O reaction showed a slight difference in conversion (at times < 30 min, which is within the experimental error); afterward, the conversion is the same in both experiments. Usually, three separate regions can be distinguished in the conversion−time curves; this is in accordance with the experimental data obtained in this work. The first interval is localized in the conversion range 0−15%, interval II within 15−52%, and interval III at conversions above 52%.[1−3] In intervals I and II of the batch process, monomer droplets act as reservoirs. The monomer diffuses from the droplets to the locus of polymerization with a rate controlled by free radical propagation. The conversion is close to 98% in both experiments. These results were validated with a gravimetric method. The polymer was precipitated by isopropanol and subsequently washed by ethanol to eliminate remaining small molecules. The dried polymer was weighted to calculate the conversion, based on a simple mass balance equation. The conversions were 96% and 92% for water and D_2O reactions, respectively. These discrepancies are associated with the loss of polymer during the precipitation process and are considered as experimental error.

The number of polymer particles at time t, $N_p(t)$, is given by eq 8 (see also[1]),

$$N_p(t) = \frac{6[M_0]X(t)}{\pi\rho_p {D_v}^3} \tag{8}$$

where $[M_0]$ is the monomer concentration, X the conversion, ρ_p the polymer density, and finally D_v is the average diameter of the latex particle.[1]

The number of polymer particles N_p produced in the course of reaction can be calculated for both reactions (water and D_2O). N_p increases with time up to ca. 75 min, and then it decreases slightly at the end of reactions (high conversion). The order of magnitude of N_p is 10^{19} dm^{-3} for both experiments. The rate of polymerization is not expected to be influenced appreciably by the number of polymer particles in a first-order kinetic system. It was shown previously that the steady-state rate of polymerization is practically independent of the number of polymer particles in case of BA polymerization using a constant surfactant concentration.[1−3] These model predictions are in accordance with our experimental data.

The rate of polymerization R_p with a maximum of $R_{p,max} = 0.1$ mol dm^{-3} min^{-1} was determined from the conversion and is depicted in Figure 5 for both experiments.[5,8,23,25,26] For the calculation of the steady-state rate of polymerization, conversions between 15 and 52% were considered as they account for the interval II kinetics. Additionally, the rate of polymerization in interval II as a function of the number of particles was proportional to $N_p^{0.97}$ and $N_p^{0.94}$ for water- and D_2O-based reactions, respectively. According to Smith−Ewart (SE) theory in interval II, R_p follows the equation $R_p \propto N_p^{1.0}$, which is in agreement with the present experimental findings.

On the other hand, the experimentally determined rate can be used to calculate the average number of radical per particle, $\tilde{n}$, using the generalized SE equation[1,4,8,23−25,29,30]

$$R_p(t) = k_p[M_p]\tilde{n}(t)\frac{N_p(t)}{N_A} \tag{9}$$

where R_p is the rate of polymerization, k_p is the rate constant for propagation in the latex particles, $[M_p]$ is the monomer concentration in the particles, N_p is the number of polymer particles, and N_A is the Avogadro number. For the calculation of $\tilde{n}$, the values for k_p and $[M_p]$ are to be known. $[M_p]$ was determined from the intersection of the drop in rate and the steady state (Figure 5). This point corresponds to the disappearance of monomer droplets and represents the transition from interval II to interval III. The conversions, at which the transition occurred, were found to be around 52%. k_p was obtained from literature. In fact, the radical number is a model-based quantity whose magnitude is strongly dependent on the assumed k_p value.[36] A large average number of free radicals per particle ranging from 3 to 9 have been reported for seeded emulsion polymerization of BA.[25] In other cases,[1−3] $\tilde{n}$ is below 0.50. This results in instantaneous termination and latex particles with either zero or one radical.

The average number of radicals per particle $\tilde{n}$ as calculated as a function of conversion is shown in Figure 6; $\tilde{n}$ decreases at higher conversions. The values of $\tilde{n}$, extracted from the NMR data, are well below 0.5, suggesting that the assumption of instantaneous termination may be applicable.[1,23−25,34] According to these data, it can be concluded that butyl acrylate polymerization can be described by zero−one kinetics. If this system is governed by zero−one kinetics, the slope and interception procedure may be used to determine entry and exit rate coefficients of radicals.

4.3. Rate-Determining Parameters in the Zero−One Seeded Emulsion Polymerization of Butyl Acrylate. The definition of a zero−one system (that a radical entering into a droplet causes rapid termination of the polymerization within the droplet) can be restated: Entry of a radical into a

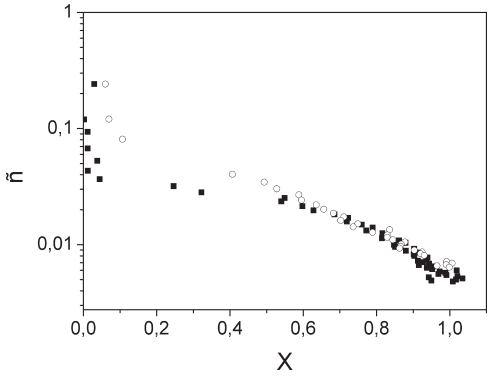

Figure 6. Variation of the average number of radicals per particle ($\tilde{n}$) as a function of conversion X for both the doubly deionized H_2O (■) and the D_2O (○) reaction. As $\tilde{n}$˜ is smaller than 0.5, a zero−one kinetics can be assumed.

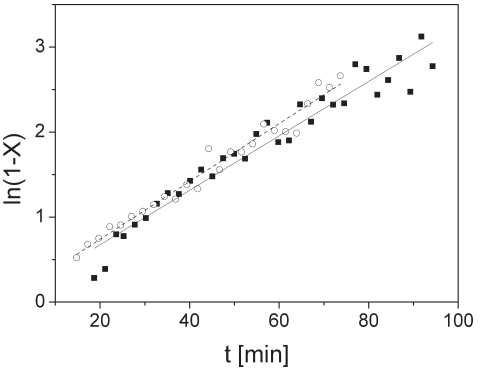

Figure 7. ln(1 − X) versus reaction time for the seeded emulsion polymerization of butyl acrylate, X being the conversion: (■) water and (○) D_2O. A linear dependence of ln(1 − X) on t is found such that from the slope the entry coefficient ρ and from the intercept the termination coefficient k can be obtained.

particle which already contains a growing polymer chain will lead to reaction termination with a high probability before significant new polymer or chain growth is formed. It is essential to provide experimental evidence that the experimental conditions chosen here indeed are compatible with zero−one kinetics (Smith−Ewart theory[23−25,36]). Another necessary but not sufficient condition is that the value of $\tilde{n}$, the average number of radicals per particle, should not exceed 0.5, which was already shown to be fulfilled in the present case.

The radical entry rate coefficient ρ is determined by the generation rate of oligomeric radicals in the aqueous phase, capable of entering a latex particle irreversibly. The exit (k) of radicals from a particle can occur by the transfer of the radical activity to a small species that is capable of diffusing away from the particle quickly. This species is normally a monomer. Once the transfer to the monomer has occurred, the monomeric radical has in principle three possible fates: (1) escape from the latex particle, (2) termination with another radical, and (3) propagation, after which escape is assumed to be impossible. The last option has no direct influence on the radical concentration in the particle in a zero−one system and is therefore kinetically unimportant.

A theoretical expression for the variation of the conversion within a certain time in a zero−one system is given by[23−25,36]

$$\ln\left[\frac{1-X(t)}{1-X_0}\right] = \frac{A}{2\rho+k}\left[\rho t+\left(\tilde{n}_0-\frac{\rho}{2\rho+k}\right)(1-\exp(-t(2\rho+k)))\right] \quad (10)$$

where X_0 is the fractional conversion at $t = 0$ and A is called conversion factor. $\tilde{n}_0$ is the radical concentration in a particle at $t = 0$. At long reaction times the equation can be simplified according to

$$\ln\left[\frac{1-X(t)}{1-X_0}\right] = \frac{A}{2\rho+k}\left[\rho t+\left(\tilde{n}_0-\frac{\rho}{2\rho+k}\right)\right] \quad (11)$$

This equation can be represented by

$$\ln\left[\frac{1-X(t)}{1-X_0}\right] = a+bt \quad (12)$$

The intercept a and the slope b of the linear equation can be obtained from the experimental data (Figure 7). The polymerization rate is constant within the interval II in a zero−one system, as evidenced by $X(t)$ being linear for a substantial time period. Thus, slope and intercept can be used to calculate ρ and k.[23−25,36] The two coefficients are

$$\rho = \frac{b}{a}\left(\tilde{n}_0-\frac{b}{A}\right) \quad (13)$$

$$k = \left(\frac{A}{a}-2\frac{b}{a}\right)\left(\tilde{n}_0-\frac{b}{A}\right) \quad (14)$$

$\tilde{n}_0$ is the initial value of $\tilde{n}$ at $t = 0$.

This technique demonstrates that both rate coefficients can be obtained with a minimum of model-based assumptions. Entry and exit rate coefficients were $\rho = 2.4 \times 10^{-4}$ s^{-1} and $k = 3.3 \times 10^{-3}$ s^{-1}, respectively. The accuracy of rate coefficients from entry and exit is mainly determined by the accuracy of k_p. Here k_p was presumed to be know exactly,[1,23−25] 450 dm^3 mol^{-1} s^{-1}. The values are consistent with those from the literature.

4.4. Modeling of the Experimental Data by the Entry Kinetic Model. As during reaction integrals and line widths change in the olefinic and in the aliphatic spectral regions, these data are analyzed by modeling via the kinetic model introduced above.[35] It is obvious that the olefinic signal decreases in both reactions, which corresponds to total amount of monomers in the reactor. However, the model assumes a constant monomer concentration in the aqueous phase, which cannot be measured directly. From the numerical simulation it is found that the intermediate states of the oligomer formation exhibit concentrations near zero for the rate coefficients known in the literature. Therefore, the reduction of the total monomer concentration is related directly to the increasing [M_3^0], and consequently, theoretical prediction and experimental result can be compared (Figure 8a,b). For numerical integration the rate coefficients summarized in Table 2 were used. The maximum number of monomer units for propagation outside the latex particle was three. This parameter set was used for both reactions. The data of the D_2O-based reaction (Figure 8b) can be described sufficiently good, allowing a direct comparison with theoretical modeling. An insensitivity of the model toward ρ_w was found which can be assumed in the range of 10^{-3}−10^{-5} s^{-1} equally well. Only a small decrease of [M_3^0] was found at large reaction times. As the olefinic concentration is no longer accurately determined at the late stages of the experiments, no definitive answer can be given from this second approach.

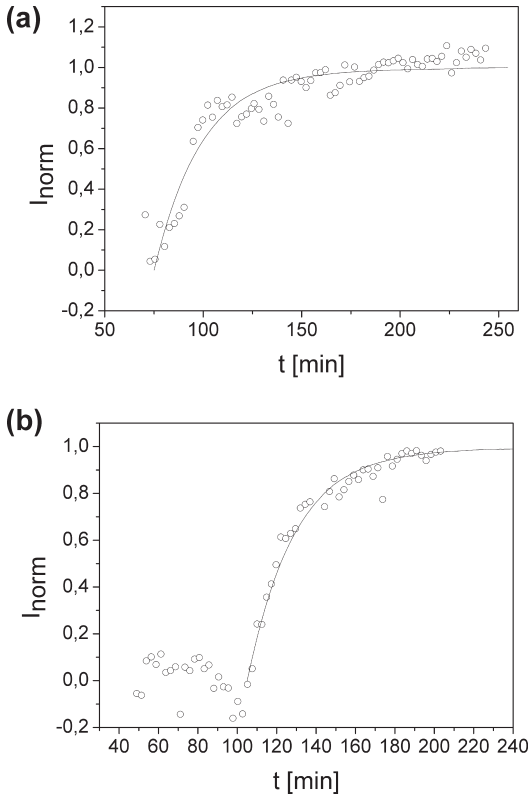

Figure 8. Normalized, reversed signal integral of the olefinic spectral region together with the result of the numerical integration of the kinetic model for the 3-mer radical $[M_3^0]$ (black lines). The parameters are given in the text and are for both reactions the same: (a) doubly deionized water-based reaction; (b) D_2O reaction. The kinetic model is found to describe the data very well within the experimental error.

Table 2. Parameters and Their Values Taken from the Literature and from the Present Work for the Emulsion Polymerization of Butyl Acrylate at 70 °C

parameter	reference
$r_s = 103$ nm	23
$D_w = 1 \times 10^{-10}$ m^2 s^{-1}	23
$[M_{aq}] = 6 \times 10^{-3}$ mol/dm^3	25
$\rho_m = 0.869$ g cm^{-3}	25
$\rho_p = 1.026$ g cm^{-3}	25
$k_p = 450$ dm^{-3} mol^{-1} s^{-1}	23, 25
$k_{tw} = (6-30) \times 10^7$ dm^{-3} mol^{-1} s^{-1}	25
$k_d = 1.3 \times 10^{-6}$ s^{-1} ($T = 50$ °C, pH = 7)	25
$\rho_w = 7.9 \times 10^{-5}-1.3 \times 10^{-3}$ s^{-1}	43
$k = 3.3 \times 10^{-3}$ s^{-1}	this work
$\rho = 2.4 \times 10^{-4}$ s^{-1}	this work
$k_d = 8 \times 10^{-4}$ s^{-1} ($T = 70$ °C)	this work
$k_{pw,ini} = 450$ dm^3 mol^{-1} s^{-1} ($T = 70$ °C)	this work
$k_{tw} = 3 \times 10^4$ dm^3 mol^{-1} s^{-1} ($T = 70$ °C)	this work
$N_p = 10^{19}$ dm^{-3} ($T = 70$ °C)	this work
$\rho_w = 10^{-5}-10^{-3}$ s^{-1} ($T = 70$ °C)	this work
$k_{p,app} = (7.7-10) \times 10^{-4}$ s^{-1} ($T = 70$ °C)	this work

Even in the DDI water-based reaction, the olefinic signal (Figure 8a) could be modeled while using the same parameter set such that an agreement with the prediction can be found. The differences in temporal behavior and in the accuracy are mainly due to the inaccuracy of the fit on the spectra. Nevertheless, the new experimental method of online low-field NMR spectroscopy can provide direct insight into the emulsion polymerization of BA.

Additionally, the apparent polymerization rate coefficient for the reaction inside the latex particles can be extracted from the change of line width with reaction time (Figure 9).

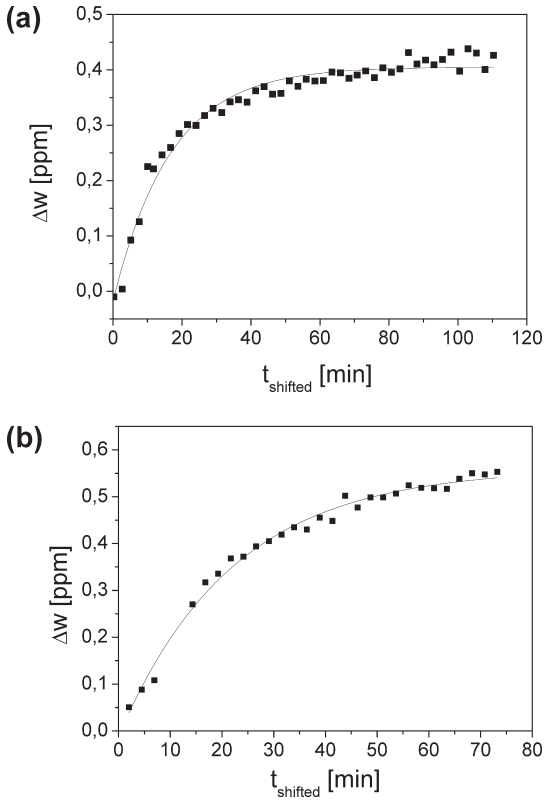

Figure 9. Increase of the line width in the aliphatic spectral region: (a) doubly deionized water-based reaction; (b) D_2O-based reaction. The apparent rate coefficients are determined within a pseudo-first-order kinetic model to 9.97×10^{-4} and 7.6×10^{-4} s^{-1}, respectively. The fit to the data is also shown in the figures (black lines).

They amount to $(7.7-10) \times 10^{-4}$ s^{-1}. The values were found by a fit of the exponentially increasing function for a pseudo-first-order reaction. Interesting to note that the increase in line width starts about 50 min later compared to the decrease of the intensity of the olefinic signal which reflects the total monomer concentration. This indicates that the polymerization reaction inside the latex particles requires a sufficient concentration $[M_3^0]$ and a sufficient chain length for effectively being observed in the NMR line width.

5. Conclusions

The emulsion polymerization of *n*-BA can be successfully monitored by online low-field ^{1}H NMR spectroscopy. This new analytical method provides useful insight into the quantitative assessment of emulsion polymerizations. Using these results, it was possible to evaluate the monomer concentrations during the reaction of butyl acrylate under batch conditions and calculate characteristic parameters like reaction rates as a function of reaction time.

The maximum rate $R_{p,max}$ is attributed to the increased number of polymer latex particles. The following decreasing of polymerization rate results from the depressed transfer of monomer from the monomer droplets to the reaction loci inside the latex particles. It is also found that the number of polymer particles increases with conversion. These findings are consistent with the literature.

The average number of radical per particle ($\tilde{n}$) is found to be much lower than 0.5, which indicates that a zero−one kinetics model can be applied for modeling the NMR data. From this approach, the exit rate constant k as well as the entry parameter ρ can be determined. Especially the propagation constant is found to be consistent with the literature value of 450 dm^3 mol^{-1} s^{-1}. Moreover, the observed line broadening can be used for the

estimate of polymerization rate inside the latex particles within a pseudo-first-order reaction scheme.

A simulation of a kinetic entry model in the aqueous phase allows a good description of the experimental findings, revealing a complete parameter set for the description of the reaction in the aqueous phase.

The online low-field NMR spectroscopy is capable of monitoring a polymerization reaction and thereby revealing valuable information about the kinetic parameters.

Acknowledgment. The "Shared Research Group 10-2" received financial support by the "Concept for the future" of Karlsruhe Institute of Technology (KIT) within the framework of the German Excellence Initiative. M.V. acknowledges the financial support by the DAAD. M. Wilhelm and C. Klein are acknowledged for valuable discussions.

References and Notes

(1) Sajjadi, S.; Brooks, B. W. *J. Polym. Sci., Part A: Polym. Chem.* **1999**, *37*, 3957–3972.
(2) Sajjadi, S.; Brooks, B. W. *J. Polym. Sci., Part A: Polym. Chem.* **1999**, *74*, 3094–3110.
(3) Sajjadi, S.; Brooks, B. W. *J. Polym. Sci., Part A: Polym. Chem.* **2000**, *38*, 528–545.
(4) Thickett, S. C.; Gilbert, R. G. *Polymer* **2007**, *48*, 6965–6991.
(5) Capek, I. *Macromol. Chem. Phys.* **1994**, *195*, 1137–1146.
(6) Reimers, J. L.; Schork, F. J. *J. Appl. Polym. Sci.* **1996**, *60*, 251–262.
(7) Buback, M. *J. Polym. Sci., Part C: Polym. Lett.* **1988**, *26*, 293–297.
(8) Chern, C. S. *Prog. Polym. Sci.* **2006**, *31*, 443–486.
(9) Ballard, M. J.; Gilbert, R. G.; Napper, D. H. *J. Polym. Sci., Polym. Lett. Ed.* **1981**, *19*, 533–537.
(10) Maiwald, M.; Fischer, H. H.; Kim, Y.-K.; Hasse, H. *J. Magn. Reson.* **2004**, *166*, 135–146.
(11) Hua, H.; Dubé, M. A. *Polymer* **2001**, *42*, 6009–6018.
(12) Fevotte, G.; Barudio, I.; Mckenna, T. F. *Comput. Chem. Eng.* **1996**, *20*, 581–586.
(13) Hiller, W.; Pasch, H.; Macko, T.; Hofmann, M.; Ganz, J.; Spraul, M.; Braumann, U.; Streck, R.; Mason, J.; Van Damme, F. *J. Magn. Reson.* **2006**, *183*, 290–302.
(14) Maiwald, M.; Fischer, H. H.; Kim, Y.-K.; Hasse, H. *Anal. Bioanal. Chem.* **2003**, *375*, 111–1115.
(15) Abdollahi, M.; Sharifpour, M. *Polymer* **2007**, *48*, 25–30.
(16) Fevotte, G.; Barudio, I.; Guillot, J. *Thermochim. Acta* **1996**, *289*, 223–242.
(17) Almamad, B.; Romagnoli, J. A.; Gomes, V. G. *Chem. Eng. Sci.* **2005**, 6596–6606.
(18) Zhang, Z. *Macromol. Symp.* **2009**, *282*, 111–127.
(19) Hiller, W.; Sinha, P.; Pasch, H. *Macromol. Chem. Phys.* **2007**, *208*, 1965–1978.
(20) Landfester, K.; Spiegel, S.; Born, R.; Spiess, H. W. *Colloid Polym. Sci.* **1998**, *276*, 356–361.
(21) Nordon, A.; Diez-Lazaro, A.; Wong, C. W. L.; McGill, C. A.; Littlejohn, D.; Weerasinghe, M.; Mamman, D. A. *Analyst* **2008**, *133*, 339–347.
(22) Horri, F.; Kaji, H.; Kuwabara, K.; Masuda, K.; Tai, T. *J. Mol. Struct.* **1998**, *441*, 303–311.
(23) Mallya, P.; Plamthottam, S. S. *Polym. Bull.* **1989**, *21*, 497–504.
(24) Zirkzee, H. F.; Van den Enden, M. J. W. A.; Van Kilsdonk, W. T.; van Herk, A. M.; German, A. L. *Acta Polym.* **1996**, *47*, 441–449.
(25) Maxwell, I. A.; Napper, D. H.; Gilbert, R. G. *J. Chem. Soc., Faraday Trans.* **1987**, *83*, 1449–1467.
(26) Özdeger, E.; Sudol, E. D.; El-Aasser, M. S.; Klein, A. *J. Polym. Sci., Part A: Polym. Chem.* **1997**, *35*, 3827–3835.
(27) Ahmad, N. M.; Heatley, F.; Lovell, P. A. *Macromolecules* **1998**, *31*, 2822–2827.
(28) Ghielmi, A.; Storti, G.; Morbidelli, M. *Chem. Eng. Sci.* **2001**, *56*, 937–943.
(29) Maeder, S.; Gilbert, R. G. *Macromolecules* **1998**, *31*, 4410–4418.
(30) Plessis, C.; Arzamendi, G.; Leiza, J. R.; Schoonbrood, H. S.; Charmot, D.; Asua, J. M. *Ind. Eng. Chem. Res.* **2001**, *40*, 3883–3894.
(31) Plessis, C.; Arzamendi, G.; Leiza, J. R.; Schoonbrood, H. A. S.; Charmot, D.; Asua, J. M. *Macromolecules* **2000**, *33*, 5041–5047.
(32) Plessis, C.; Arzamendi, G.; Leiza, J. R.; Schoonbrood, H. A. S.; Charmot, D.; Asua, J. M. *Macromolecules* **2000**, *33*, 4–7.
(33) Capek, I.; Juranicova, V.; Barton, J. *Polym. Int.* **1997**, *43*, 1–7.
(34) Buback, M.; Deneger, B. *Makromol. Chem.* **1993**, *194*, 2875–2883.
(35) Maxwell, I. A.; Morrison, B. R.; Napper, D. H.; Gilbert, R. G. *Macromolecules* **1991**, *24*, 1629–1640.
(36) Hawkett, B. S.; Napper, D. H.; Gilbert, R. G. *J. Chem. Soc., Faraday Trans. 1* **1980**, *76*, 1323–1343.
(37) Scheren, P. A. G. M.; Russell, G. T.; Sangster, D. F.; Gilbert, R. G.; German, A. L. *Macromolecules* **1995**, *28*, 3637–3649.
(38) Coen, E. M.; Peach, S.; Morrison, B. R.; Gilbert, R. G. *Polymer* **2004**, *45*, 3595–3608.
(39) Casey, B. S.; Morrison, B. R.; Maxwell, I. A.; Gilbert, R. G.; Napper, D. H. *J. Polym. Sci., Part A: Polym. Chem.* **1994**, *32*, 605–630.
(40) Russell, G. T.; Gilbert, R. G.; Napper, D. H. *Macromolecules* **1992**, *25*, 2459–2469.
(41) Lyons, R. A.; Hutovic, J.; Piton, M. C.; Christie, D. I.; Clay, P. A. *Macromolecules* **1996**, *29*, 1918–1927.
(42) Russell, G. T. *Macromolecules* **1993**, *26*, 3538–3552.
(43) Morrison, B. R.; Casey, B. S.; Lacik, I.; Leslie, G. L.; Sangster, D. F. *J. Polym. Sci., Polym. Chem.* **1994**, *32*, 631–649.